LETTERS

Imaging and dynamics of light atoms and molecules on graphene

Jannik C. Meyer[1,2], C. O. Girit[1,2], M. F. Crommie[1,2] & A. Zettl[1,2]

Observing the individual building blocks of matter is one of the primary goals of microscopy. The invention of the scanning tunnelling microscope[1] revolutionized experimental surface science in that atomic-scale features on a solid-state surface could finally be readily imaged. However, scanning tunnelling microscopy has limited applicability due to restrictions in, for example, sample conductivity, cleanliness, and data acquisition rate. An older microscopy technique, that of transmission electron microscopy (TEM)[2,3], has benefited tremendously in recent years from subtle instrumentation advances, and individual heavy (high-atomic-number) atoms can now be detected by TEM[4–7] even when embedded within a semiconductor material[8,9]. But detecting an individual low-atomic-number atom, for example carbon or even hydrogen, is still extremely challenging, if not impossible, via conventional TEM owing to the very low contrast of light elements[2,3,10–12]. Here we demonstrate a means to observe, by conventional TEM, even the smallest atoms and molecules: on a clean single-layer graphene membrane, adsorbates such as atomic hydrogen and carbon can be seen as if they were suspended in free space. We directly image such individual adatoms, along with carbon chains and vacancies, and investigate their dynamics in real time. These techniques open a way to reveal dynamics of more complex chemical reactions or identify the atomic-scale structure of unknown adsorbates. In addition, the study of atomic-scale defects in graphene may provide insights for nanoelectronic applications of this interesting material.

The atomic-scale resolution of TEM comes at the price of requiring that the transmitted electron beam reach the imaging lenses and detector, and so TEM works only for ultra-thin, electron-transparent samples. In high-resolution TEM and all related techniques—such as electron diffraction, scanning transmission electron microscopy, electron energy loss spectroscopy or elemental mapping—any support film or membrane provides a background signal that is most significant for the smallest objects under investigation. Individual nanoscale particles or molecules usually need to be supported by a continuous membrane, as only tubular or rod-shaped nanoparticles (such as carbon nanotubes) can be suspended across holes in the membrane. Indeed, single-walled carbon nanotubes have been used for low-background TEM studies of encapsulated molecules[13–15] or of defects in the cylinder-shaped graphene sheets[16,17]. However, the limited space, harsh filling procedures, and strongly curved shape of the sheet limit the applicability and complicate the analysis.

As we demonstrate below, a graphene membrane provides the ultimate sample support for electron microscopy. With a thickness of only one atom, it is the thinnest possible continuous material. Owing to its crystalline nature, a graphene support membrane is either completely invisible or, if the graphene lattice is resolved by a very-high-resolution microscope, its contribution to the imaging signal can be easily subtracted. Graphene is also a good electrical conductor and therefore displays minimal charging effects from the electron beam. Remarkably, we find that a graphene membrane enables single-adatom sensitivity even when using a common TEM that does not resolve a graphitic lattice.

In order to observe adsorbates at the single-atom level, the graphene support membrane must be exceptionally clean. In contrast to an earlier graphene membrane preparation method[18], our approach does not rely on electron beam lithography and is simple enough to be reproducible in any basic microscopy laboratory (a detailed description of the sample preparation is given in the Supplementary Information). In brief, we start with graphene prepared by mechanical cleavage with an adhesive tape[19–21], and transfer selected sheets to commercially available TEM grids. We use electron diffraction analysis[18] to verify the presence of a single layer. Figure 1a shows a low-magnification view of a graphene sheet suspended across the 1.3 μm holes of the perforated carbon foil, with a close-up shown in Fig. 1b. More than 50% of the area on these graphene membranes appears exceptionally clean, with no dramatic contrast in high-resolution TEM images (Fig. 1b). As we now demonstrate, however, these 'clean' regions contain individual adatoms that are readily observable by TEM. Although individual exposures can reveal useful data, a dramatic improvement in the signal-to-noise ratio is achieved by summing multiple subsequent frames (corrected for sample drift), which effectively increases the exposure time beyond the dynamic range of the TEM CCD detector. Summing as few as five frames yields striking visual improvement with atomic-scale features (including individual adatoms) becoming readily apparent, and summing 100 frames reduces the noise to below 0.12% (standard deviation in a relatively featureless region of the graphene membrane).

Figure 2a shows a TEM image in which an individual carbon atom, attached to the graphene membrane, is identified by an arrow. We recorded eight consecutive images essentially identical to that of Fig. 2a (each a summation of 20 frames on the CCD), demonstrating that the carbon atom did not adsorb or desorb during the time of exposure. To identify the adatom, image simulations were carried out as described in the Supplementary Information. The good agreement between the TEM data and image simulation (Fig. 2b, c) confirms the carbon atom identification. Simulations for individual boron, nitrogen or oxygen adatoms also provide reasonable fits; however, carbon is the dominant component of vacuum contamination and surface adsorbates within our TEM, making these other candidates unlikely.

Closer inspection of Fig. 2a also reveals faint atomic-scale structure distinctly different from carbon adatoms. To highlight these faint features, we show in Fig. 2d a summation of 100 consecutive TEM frames for the same physical region. Figure 2d reveals a moderate density of additional dark features (dark grey points, a selection of

[1]Department of Physics, University of California at Berkeley, Berkeley, California 94720, USA. [2]Materials Sciences Division, Lawrence Berkeley National Laboratory, Berkeley, California 94720, USA.

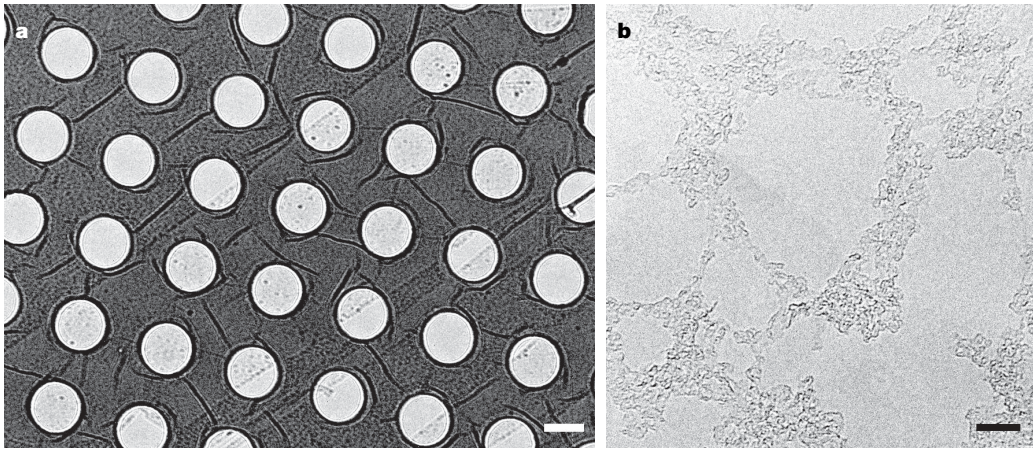

Figure 1 | Graphene membrane sample as observed by TEM. a, Low-magnification overview image of a suspended graphene sheet on the perforated carbon foil. **b**, High-resolution close-up of a graphene membrane. We observe small, extremely clean areas with diameters of 10–50 nm where no contrast is visible, separated by regions with thin amorphous adsorbates. Scale bars; 1 μm (**a**), 10 nm (**b**).

which are identified with red arrows) with identical intensity profiles, all with a central dip reduction near 0.6% of the mean bright-field intensity (Fig. 2e). By comparing the TEM image data for these additional features to adatom simulations, we rule out any adatom heavier than helium, as well as a substitution of carbon atoms in the graphene membrane by other elements. However, a hydrogen adatom results in the correct 0.6% dip in the bright-field intensity, shown by the red curve in Fig. 2e. The large number of essentially identical adatom profiles, along with the excellent agreement with the simulated contrast, provides convincing evidence that we have, for the first time to our knowledge, detected individual hydrogen atoms by TEM.

We emphasize that we do not claim to have resolved a hydrogen–carbon distance, which would require advanced aberration-corrected instrumentation. However, detecting an isolated hydrogen atom against a nearly invisible background only requires an adequate signal-to-noise ratio. Electron scattering from hydrogen has been detected previously in electron diffraction experiments[22], and was found to produce a three to four times lower signal than carbon, in agreement with our values. In order to verify the uniqueness of the hydrogen atom identification, we consider whether alternative structures may lead to the observed contrast. The contrast match to simulations, using edges or vacancies in the sheet as reference, is better than a factor of two (see Supplementary Information) in our experiment. For an adatom on the sheet, only hydrogen or helium can produce the observed contrast. We rule out helium, as it will not bind to carbon and is not present anywhere in the experiment. We considered all known defects of graphene sheets. All vacancies, relaxed[23] or not, will produce a white spot. An adatom–vacancy pair[16], even with the minimum separation below the resolution of our microscope, would show a white-and-black symmetric intensity at a detectable level according to simulations, and was indeed observed. A Stone–Wales defect[23] is also expected to have a white-and-black symmetric contrast with zero mean value. Extended defects, such as dislocations, would not produce the rotationally symmetric contrast of an adatom. Finally, a single-layer graphene

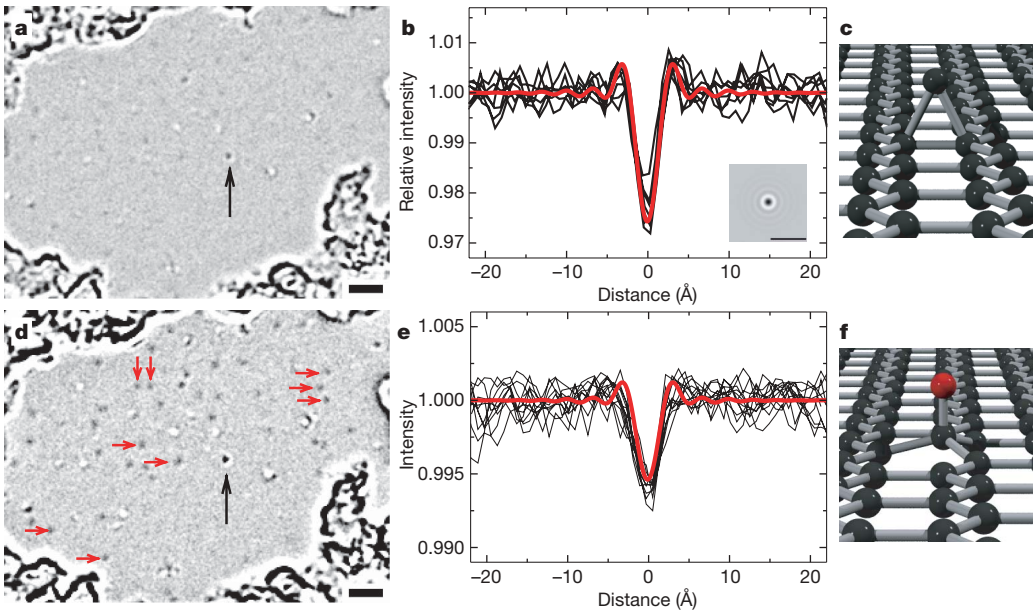

Figure 2 | Adatom images. a, Carbon adatom (indicated by black arrow). **b**, Intensity profiles from several images of the carbon adatom (black traces), and a simulated profile (red trace). Inset, simulated image. **c**, Carbon adatom configuration according to ref. 30. **d**, Hydrogen adatoms on the same sample (dark grey spots), a selection of which are indicated by red arrows. Black arrow again indicates the carbon adatom. **e**, Profile plots of selected hydrogen adatoms from **d** (black traces). Red line is the simulated profile for a hydrogen adatom. **f**, Configuration of a chemisorbed hydrogen atom (red) according to ref. 25. All scale bars, 2 nm.

membrane has a much smaller set of possible defects than graphite (or few-layer graphene): for example, it can not have interstitials or bonds between layers. Thus, we confirm the identification of the hydrogen adatom.

In addition to individual adatoms, we observe by the same TEM imaging methods the generation (by the electron beam) and dynamics of defects (vacancies) in the graphene membrane, as well as the dynamics of a variety of molecular-scale adsorbates. The formation of vacancies owing to knock-on damage by the electron beam is shown in Fig. 3a–c. We also observe vacancies that disappear by interaction with mobile adsorbates. Larger adsorbates (small molecules) become trapped preferentially at defects, and can be observed at one position for typically one to five minutes. Frequently, we see that the vacancy disappears along with the trapped adsorbate (Fig. 3d–f), and the missing carbon atom has obviously been resubstituted from the adsorbate. Further, we can directly observe linear molecules on graphene membranes (Fig. 4) that resemble an individual alkane or alkene carbon chain. These molecules are found to spontaneously appear in the field of view, presumably adsorbed onto the graphene membrane from the vacuum contamination. We can follow their dynamics for several minutes, as shown in Fig. 4b–d and in the Supplementary Videos.

The remarkable TEM imaging capability afforded by a suspended, single graphene membrane warrants further discussion. For an ideal graphene sheet, there are no components in the structure with a period larger than 2.1 Å, which is beyond the information limit of approximately 2.9 Å for the microscope used in the present studies (JEOL 2010 operated at 100 kV). Therefore, although the ideal graphene membrane cannot be resolved under these conditions, any perturbation to the crystalline structure can be detected as long as a sufficient number of electrons can be recorded for statistical significance. Indeed, our graphene membranes are highly stable in the electron beam at 100 kV, allowing long data collection times on one region. For example, all images in Figs 2–4 are recorded from graphene membranes after between one and three hours of irradiation (at $\sim$7 A cm^{-2}). Moreover, the summation of 100 consecutive CCD frames corresponds to an exposure time of 20 min, and distortions in the membrane during this time are below the resolution limit. This combination of a crystalline, atomically thin membrane along with the high beam stability and the absence of an amorphous background signal on the nominally clean membrane enables this unprecedented single-light-atom sensitivity in TEM. In comparison, single-walled carbon nanotubes show strong deformations under the same dose and energy of electron irradiation (see figure 5 of ref. 24), probably because the cylindrical geometry allows beam-induced defects to relax via local deformations more easily.

The observation of stable and well-localized hydrogen adatoms on graphene, in spite of the irradiation and room temperature conditions, implies that these are chemisorbed rather than physisorbed atoms. Strong bonding of hydrogen to graphite is possible if the nearest carbon atom changes its bonds from sp^2 to sp^3 configuration[25–27], with the carbon atom displaced from the plane by about 0.36 Å (Fig. 2f). Moreover, it was found[25] that hydrogen cannot bind to graphene if the carbon is confined to a plane (for example by strong bonding to a substrate), whereas an isolated membrane can deform easily to accommodate different types of bonds[28,29]. From the observed density of hydrogen adatoms, we conclude that only about 0.3% of the carbon atoms in our graphene membrane are in an sp^3 configuration with a hydrogen adatom.

Our real-time observation of molecular dynamics has important implications for chemical diffusion and reaction dynamics studies. As demonstrated above, a variety of molecular-scale adsorbates become trapped on the membrane, and often detach again or decompose after a few minutes. We can observe individual alkane-type molecules and we can even follow their migration. Alkanes are an essential ingredient of organic chemistry, and it therefore appears likely that other, more complex, molecules could be observed after deposition on graphene membranes. We find that the carbon chains are sufficiently stable and localized for characterization even at room temperature, and note that these adsorbates were only trapped on the membrane after a moderate density of defects had been created by irradiation.

In conclusion, we have demonstrated that graphene membranes enable TEM visualization of ultra-low-contrast objects. The imaging of individual hydrogen and carbon adatoms and carbon chains demonstrates a new level of sensitivity that is relevant for organic materials. A key strength of the TEM is its ability to image individual entities rather than averaging over an ensemble, and direct imaging promises insights ranging from the characterization of complex chemicals and nanomaterials to biological molecules. The extremely high sensitivity that a graphene membrane in the TEM provides with

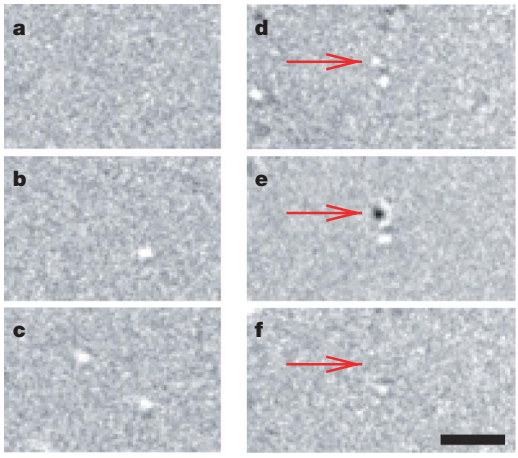

Figure 3 | Dynamics of defects. **a–c**, Generation of vacancies owing to electron irradiation. Time between **a** and **c** is 50 min. **d–f**, Annealing of a vacancy by interaction with an adsorbate. We observe two individual vacancies (**d**), and then trapping of a larger adsorbate (**e**), corresponding to a mass of a few carbon atoms, on one of the defects. After $\sim$5 min, both the adsorbate and one vacancy disappear (**f**), showing that the missing carbon atom in the graphene sheet has been replaced by an atom from the adsorbate. Scale bar, 2 nm.

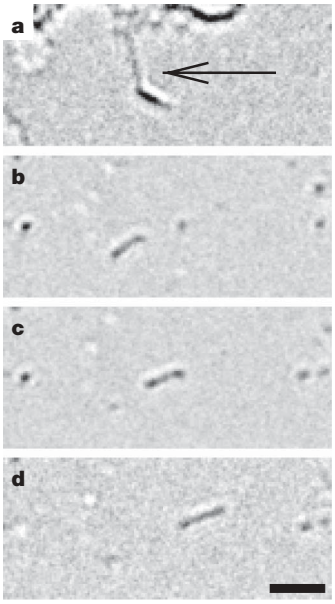

Figure 4 | Molecular scale adsorbates. **a**, Molecule suspended between other adsorbates (arrow). **b–d**, Migration of a carbon chain, where one end remains attached in each step. This migration is also shown in the Supplementary Video. The contrast is in agreement with an alkane molecule. Scale bar, 2 nm.

respect to adsorbates has allowed us to detect even hydrogen, demonstrating the ultimate in TEM atomic sensitivity. Whereas the study of defects, vacancies and edges of the graphene sheet itself will provide insights for potential electronic modifications of this new material, the placement of objects on graphene membranes will enable unprecedented analysis by TEM, including electron spectroscopic analysis, and the study of molecular dynamics.

METHODS SUMMARY

Graphene sheets are prepared on oxidized silicon substrates by mechanical cleavage. After identification by optical microscopy, selected sheets are transferred to Quantifoil TEM grids (Quantifoil Micro Tools) with 1.2 μm holes. The perforated TEM support film is brought into contact with the substrate and graphene sheet by evaporating a drop of solvent. The substrate is then removed by wet chemistry, while the graphene sheet remains attached to the TEM grids (details are given in the Supplementary Information). TEM imaging is carried out in a JEOL 2010 microscope operated at 100 kV. The sample holder is at room temperature; the actual sample temperature may differ owing to electron beam heating or the nearby decontaminator cold trap. A continuous sequence of images is recorded on the CCD camera. The defocus value (60 nm) and presence of vibrations is estimated from the thin amorphous coverage that intersperses the clean areas of the graphene membrane for each frame, and ~5% of the frames are discarded. Then, drift-compensated summations of up to 100 frames are performed (with each frame verified for imaging parameters and vibrations) to obtain an adequate signal-to-noise ratio. Orthogonal slices through the stack of images (see Supplementary Information) clearly establish whether a feature of interest has been static during the entire effective exposure time, or can be used to detect interesting dynamics in the data.

Received 10 December 2007; accepted 7 May 2008.

1. Binning, G., Rohrer, H., Gerber, Ch. & Weibel, E. Surface studies by scanning tunneling microscopy. *Phys. Rev. Lett.* **49,** 57–61 (1982).
2. Spence, J. C. H. *High-Resolution Electron Microscopy* (Oxford Univ. Press, Oxford, UK, 2003).
3. Buseck, P. R., Cowley, J. M. & Eyring, L. *High-Resolution Transmission Electron Microscopy* (Oxford Univ. Press, Oxford, UK, 1988).
4. Crewe, A. V., Wall, J. & Langmore, J. Visibility of single atoms. *Science* **168,** 1338–1340 (1970).
5. Hashimoto, H. *et al.* Visualization of single atoms in molecules and crystals by dark field electron microscopy. *J. Electron Microsc. (Tokyo)* **22,** 123–134 (1973).
6. Iijima, S. Observation of single and clusters of atoms in bright field electron microscopy. *Optik* **48,** 193–213 (1977).
7. Nellist, P. D. & Pennycook, S. J. Direct imaging of the atomic configuration of ultradispersed catalysts. *Science* **274,** 413–415 (1996).
8. Voyles, P. M., Muller, D. A., Grazul, J. L., Citrin, P. H. & Gossmann, H.-J. L. Atomic-scale imaging of individual dopant atoms and clusters in highly n-type bulk silicon. *Nature* **416,** 826–829 (2002).
9. van Benthem, K. *et al.* Three-dimensional imaging of individual hafnium atoms inside a semiconductor device. *Appl. Phys. Lett.* **87,** 034104 (2005).
10. Doyle, P. A. & Turner, P. S. Relativistic Hartree-Fock x-ray and electron scattering factors. *Acta Crystallogr. A* **24,** 390–397 (1968).
11. Kisielowski, C. *et al.* Imaging columns of the light elements carbon, nitrogen and oxygen with sub Angstrom resolution. *Ultramicroscopy* **89,** 243–263 (2001).
12. Jia, C. L., Lentzen, M. & Urban, K. Atomic-resolution imaging of oxygen in perovskite ceramics. *Science* **299,** 870–873 (2003).
13. Smith, B. W., Monthioux, M. & Luzzi, D. E. Encapsulated C in carbon nanotubes. *Nature* **396,** 323–324 (1998).
14. Liu, Z. *et al.* Transmission electron microscopy imaging of individual functional groups of fullerene derivatives. *Phys. Rev. Lett.* **96,** 088304 (2006).
15. Lui, Z., Yanagi, K., Suenaga, K., Kataura, H. & Iijima, S. Imaging the dynamic behaviour of individual retinal chromophores confined inside carbon nanotubes. *Nature Nanotechnol.* **2,** 422–425 (2007).
16. Hashimoto, A., Suenaga, K., Gloter, A., Urita, K. & Iijima, S. Direct evidence for atomic defects in graphene layers. *Nature* **430,** 870–873 (2004).
17. Suenaga, K. *et al.* Imaging active topological defects in carbon nanotubes. *Nature Nanotechnol.* **2,** 358–360 (2007).
18. Meyer, J. C. *et al.* The structure of suspended graphene sheets. *Nature* **446,** 60–63 (2007).
19. Novoselov, K. S. *et al.* Two-dimensional atomic crystals. *Proc. Natl Acad. Sci. USA* **102,** 10451–10453 (2005).
20. Novoselov, K. S. *et al.* Two-dimensional gas of massless Dirac fermions in graphene. *Nature* **438,** 197–200 (2005).
21. Zhang, Y., Tan, J. W., Stormer, H. L. & Kim, P. Experimental observation of the quantum Hall effect and Berry's phase in graphene. *Nature* **438,** 201–204 (2005).
22. Vainshtein, B. K. & Pinsker, Z. G. Opredelenie Polozheniya Vodoroda V Kristallicheskoi Reshetke Parafina. *Dokl. Akad. Nauk SSSR* **72,** 53–56 (1950).
23. Amara, H., Latil, S., Lambin, Ph. & Charlier, J.-C. Scanning tunneling microscopy fingerprints of point defects in graphene: A theoretical prediction. *Phys. Rev. B* **76,** 115423 (2007).
24. Smith, B. W. & Luzzi, E. Electron irradiation effects in single wall carbon nanotubes. *J. Appl. Phys.* **90,** 3509–3515 (2001).
25. Jeloaica, L. & Sidis, V. DFT investigation of the adsorption of atomic hydrogen on a cluster-model graphite surface. *Chem. Phys. Lett.* **300,** 157–162 (1999).
26. Sha, X. & Jackson, B. First-principles study of the structural and energetic properties of H atoms on a graphite (0001) surface. *Surf. Sci.* **496,** 318–330 (2002).
27. Hornekaer, L. *et al.* Metastable structures and recombination pathways for atomic hydrogen on the graphite (0001) surface. *Phys. Rev. Lett.* **96,** 156104 (2006).
28. Boukhvalov, D. W., Katsnelson, M. I. & Lichtenstein, A. I. Hydrogen on graphene: Electronic structure, total energy, structural distortions and magnetism from first-principles calculations. *Phys. Rev. B* **77,** 035427 (2007).
29. Ito, A., Nakamura, H. & Takayama, A. Chemical reaction between single hydrogen atom and graphene. Preprint at ⟨http://arxiv.org/abs/cond-mat/0703377⟩ 2007.
30. Nordlund, K., Keinonen, J. & Mattila, T. Formation of ion irradiation induced small-scale defects on graphite surfaces. *Phys. Rev. Lett.* **77,** 699–702 (1996).

Supplementary Information is linked to the online version of the paper at www.nature.com/nature.

Acknowledgements This work was supported by the Director, Office of Energy Research, Office of Basic Energy Sciences, Materials Sciences and Engineering Division, of the US Department of Energy under contract DE-AC02-05CH11231. A.Z. acknowledges support from the Miller Institute of Basic Research in Science, and C.O.G. acknowledges support from an NSF Graduate Fellowship.

Author Information Reprints and permissions information is available at www.nature.com/reprints. Correspondence and requests for materials should be addressed to J.C.M. (email@jannikmeyer.de) or A.Z. (azettl@berkeley.edu).